Erosion-Corrosion of Iron and Nickel Alloys at Elevated Temperature in a Combustion Gas Environment

*J.H. Tylczak**[1]

[1]*National Energy Technology Laboratory, USA*

joseph.tylczak@netl.doe.gov

Abstract

This paper reports on the results of a study that compares the erosion-corrosion behavior of a variety of alloys (Fe- 2¼Cr 1Mo, 304 SS, 310 SS, Incoloy 800, Haynes 230 and a Fe_3Al) in a combustion environment. Advanced coal combustion environments, with higher temperatures, are driving re-examination of traditional and examination of new alloys in these hostile environments. In order to simulate conditions in advanced coal combustion boilers, a special erosion apparatus was used to allow for impingement of particles under a low abrasive flux in a gaseous environment comprised of 20 % CO_2, 0.05 % HCl, 77 % N_2, 3 % O_2, and 0.1 % SO_2. Tests were conducted at room temperature and 700 °C with ~ 270 µm silica, using an impact velocity of 20 m/s in both air and the simulated combustion gas environment. The erosion-corrosion behavior was characterized by gravimetric measurements and by examination of the degraded surfaces optically and by scanning electron microscopy (SEM). At room temperature most of the alloys had similar loss rates. Not surprisingly, at 700 °C the lower chrome-iron alloy had a very high loss rate. The nickel alloys tended to have higher loss rates than the high chrome austenitic alloys.

Keywords: Erosion-Corrosion, Elevated Temperature, Combustion, Heat Exchangers, PC Boiler

1. INTRODUCTION

Erosion and erosion-corrosion are problems that can limit the availability of a variety of industrial plants and add to the cost of operation. The importance of understanding and designing for erosion combined with corrosion has resulted in many studies. Specialized conferences and symposiums have been organized and devoted to this topic; which has resulted in progress toward improved materials [1-3] and models for understanding the behavior [4]. Yet with the push for greater process efficiencies, resulting in higher

process temperature and new demands on materials performance, the need for further improvements in materials performance, characterization, and an understanding of degradation mechanisms are of paramount importance. An example is traditional pulverized coal-steam power plants have a boiler tube firewall temperature of ~ 565 °C, while the target of DOE's advance combustion power plants should have a tube firewall temperature of ~790 °C. In addition oxy-fuel combustion is being explored as a way to facilitate CO_2 sequestration. Issues such as these necessitate revisiting existing materials performance at these higher temperatures plus evaluating new materials.

In coal combustion power plants there are a variety of components subjected to erosion or erosion-corrosion, including: pipes for the transport of the coal to the boiler, the nozzles where the coal is inject into the burners, the firewalls, the heat exchange tubes, and outlet ducting where the combustion gases flow [4]. Erosion-corrosion occurs when the gas entrained coal ash impacts the boiler components in the elevated temperature combustion gas environment. This work focuses on the erosion-corrosion of heat-exchanger tube materials in a coal combustion environment.

To investigate materials resistant to the combined actions of erosion and corrosion in the laboratory, it is necessary to closely simulate the conditions found in the field. The main variables that influence erosion are the size, shape, velocity, angle of impact, composition of the eroding particles, the properties of the surface being eroded, and the temperature of the system [5-9]. The main variables that influence corrosion are the gas chemistry, the temperature of the system, and the properties of the surface being corroded [8, 10, 11]. As an added detail, it has been observed that the effect of velocity can change the process of whether corrosion is enhancing the erosion, or erosion enhancing the corrosion [12]. A number of the variables in this study were matched to the conditions within the range expected in advanced coal combustion boilers. These variables include the temperature, the velocity of the particles, and the gas chemistry. Advanced plants are proposed to produced steam at 760 °C [13]. The velocity of the eroding particles in pulverized coal power plants is about 10-40 m/s [7, 8, 14], and the gas chemistry (vol. %) is in the range of 8.5-12 CO_2, 65-72 N_2 , and 6 O_2 [15]. Minor, but highly important to corrosion, gas constituents found in coal combustion gas are HCl and SO_2. Since silica is usually the mineral in the ash that causes the most erosion [7, 8, 11, 16], silica sand was chosen as the erodent. The feed rate of the silica sand was adjusted to produce an abrasive flux of 0.033 g/(cm^2 · min), which is similar to what is found in a PC boiler. The time of the test at temperature was 120 h (5 days).

2. EXPERIMENTAL PROCEDURE

2.1 Erosion-corrosion apparatus

A special erosion-corrosion apparatus was used for this study (Fig 1) to simulate the exposure to abrasive materials and hostile environments found in heat exchangers of boilers. These components are exposed to high temperatures for extended periods of operating times with gas impingement at relatively low flow velocities (< 50 m/s). The

design of this erosion-corrosion apparatus used a whirling arm for good control of the particle velocity [17], located in an electrically heated retort. The retort is supplied with a mixed gas created by mixing pure gases which are controlled by mass flow controllers. This mixing of pure gases allows flexibility for creating test gas mixtures. The apparatus was designed to use a lower abrasive flux rate than its predecessors, in order to be more representative of the corrosion versus the erosion rates seen in practice. A more complete description of the apparatus may be found in a prior publication [18].

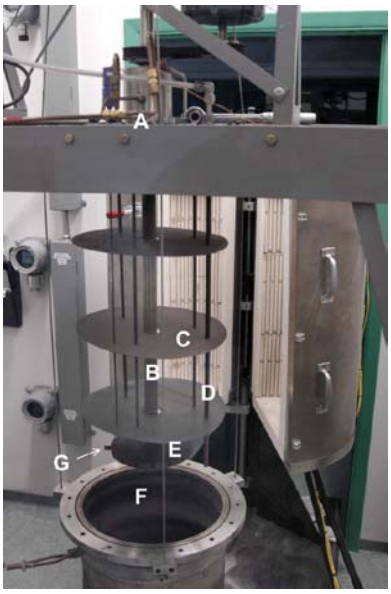

Components of HAET apparatus:

A	Lid
B	Drive shaft
C	Heat shields
D	Gas inlet/outlet tubes
E	Sample mounting disk
F	Retort
G	Test sample

Fig 1. Picture showing an overall view of the erosion-corrosion apparatus.

2.2 Environments

Tests were conducted at room and at 700 °C. At room temperature, both N_2 and air were used; and as expected, there was no difference in the results. At 700 °C tests were conducted using air and a simulated combustion atmosphere with 20 % CO_2, 0.05 % HCl, 77 % N_2, 3 % O_2, and 0.1 % SO_2. Most of the gases were introduced by metering with mass flow controllers and mixing prior to injection into the top of the retort. A portion of the N_2 was mixed with the abrasive particle feed to keep the aggressive gases out of the powder feeder. The input gases were heated as they flowed down a drop tube located in the retort. The exhaust gases were removed from near the bottom of the retort. A flow basis of one liter per minute at room temperature and atmospheric pressure was used for these tests.

2.3 Materials

In these tests a series of common boiler tube metal alloys plus some non-conventional alloys were chosen. They represent a range of common (T-22 type 2¼Cr, 1Mo steel), to high alloyed steels (304 SS, 310 SS and Incoloy 800 steels). Many of these are ASME

boiler code rated materials and are used in existing pulverized coal plants. Table 1 lists the alloys tested and their nominal composition.

	Fe	Al	C	Cr	Mn	Mo	Ni	Si	
310 Stainless steel	bal.		<0.25	24-26	<2		19-22	<1.5	
304 Stainless steel	bal.		<0.8	17.5-20	<2		8.5-10.5	<1	
2¼Cr 1Mo steel	bal.		0.12	2.25	0.45	1		0.35	
Incoloy 800	bal.	0.15-0.60	<.1	19-23	<1.5		30-35	<1	0.15-0.6 Ti
Haynes 230	3		0.10	22	0.5	2	bal.	0.4	14 W
Nitronic 30	bal.		0.03	16.0	16.0		2.25	0.3	.23 N
Fe_3Al	bal.	15							

Table 1. Alloys tested in HAET test and their mass % composition.

2.4 Specimen preparation

Each specimen was capacitive discharge welded to a 6.2 mm dia. 304 SS stub that was about 18mm long. An example of a received and prepared sample is shown in Fig 2. The stubs then had a hole drilled in them that was used to lock the specimen in the HAET specimen holder disk. After the hole was drilled the stubs were ground with abrasive paper to remove any surface oxide. Before testing the assembled samples were cleaned and mass measured to ±0.01 mg.

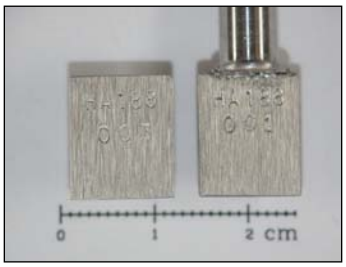

Fig 2. An example of a raw specimen and a specimen welded to mounting stub.

2.5 Test procedure

These tests used a 90 ° erodent impingement angle, normal to the surface, with an impact velocity of 20 m/s. The velocity obtained as the abrasive fell down the drop tube allowed for eight samples at a time to be attached to the mounting disk and tested. Duplicate samples of each alloy were inserted into the sample mounting disk as erosion-corrosion samples. This allowed four different alloys to be run at a time, one of which was always 310 SS. Additional samples of each alloy were hung from the bottom heat shield in an area away from the abrasive (and therefore erosion), to separate out and isolate the effect of the corrosive atmosphere. In addition to the regular corrosion samples, a blank 304 SS mounting stub was added to determine the corrosion rate of the stubs.

To run a test, the system was sealed and N_2, flowing at a rate of 2 L/min, was used to purge the system. The N_2 purge gas, and later the test atmosphere, was introduced at the top of the lid. After several hours of purging, the sample drive shaft motor was turned on. Next the furnace was turned on and brought up to 700 °C. After a hold time of 1 h, the

selected gas chemistry and the silica abrasive feed, at 0.17 g/min, were simultaneously started.

Elevated temperature HAET tests ran for 120 hrs. At that point, the furnace, environmental gases, and abrasive feed were turned off. The clamshell design furnace was removed from the retort to speed the cooling. Flowing N_2 was used as a purge as the system cooled. Once the system was cooled, it was opened and the samples were removed.

The samples were visually examined to evaluate the condition of any scale. After visual examination, the samples were cleaned. First any loose scale was intentionally removed using a soft bristle brush, followed by an ultrasonic cleaning in a soap and water mixture. The samples were then rinsed with water and dried. The stubs from uncleaned erosion-corrosion samples were initial smoother than the stubs from the corrosion samples. This is thought to be because some of the rough scale on the erosion-corrosion stubs was removed while extracting the stubs from the specimen holder. All of the stubs were additionally cleaned using a green abrasive scouring pad, after which all the stubs for that test condition appeared the same. For all analyses, the corrosion of the stubs (bare, on corrosion samples, and on erosion-corrosion samples) was assumed to be identical. After the cleaning was complete the samples mass was measured again and visually examined. The corrosion, erosion with erosion enhanced corrosion, and total erosion-corrosion loss rates were determined using gravimetric calculations.

3. RESULTS

3.1 Examination

3.1.1 Room temperature tests

The room temperature tests were configured as baseline tests. As one would expect, at room temperature there was no corrosion on any of the samples and the surface of the erosion samples showed only a roughing due to the impact of the abrasive, as illustrated in the SEM backscatter image shown in Fig 3 for a 310 SS sample. This was typical of all the alloys tested where the surface is deformed at the point of abrasive particle impact. Higher magnification secondary electron views, Fig 4, show surface platelet formation of the metal [19]. The platelets are an intermediate step in the material removal. Further impacts result in fatigue and necking of extruded cold worked metal and later removal.

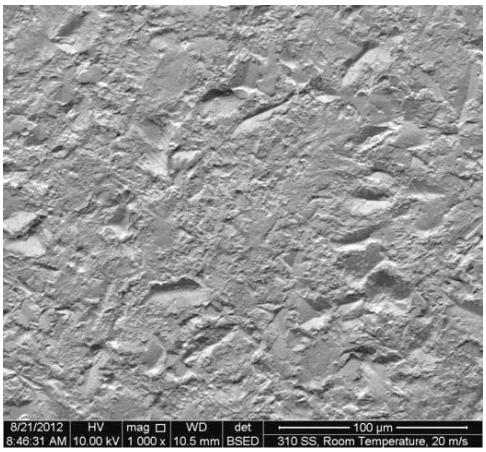

Fig 3. A worn surface of a 310 SS sample tested in the HAET apparatus at room temperature with an ~270 µm silica abrasive flux rate of 0.033 g/(cm^2·min) impacting at 20 m/s.

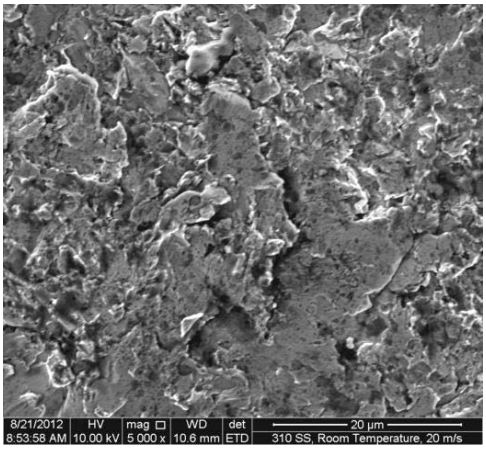

Fig 4. A secondary electron image of a 310 SS eroded surface showing platelet formation.

3.1.2 700 °C in air tests

Only a 310 SS and Haynes 230 were tested at 700 °C in air. Both the 310 SS and the Haynes 230 show substantial scaling prior to cleaning. Visually, under the easily removed outer scale, both alloys were generally smooth. SEM examination showed substantial differences. The corrosion sample of the 310 SS, Fig 5, still appeared smooth, with the original grinding marks still visible on the surface, where the erosion-corrosion surface showed a tightly adhered scale layer. The brittle scale layer showed characteristics of a roughly deformed underlining ductile metal surface, while at the surface the impact of the abrasive had left cracks in the scale.

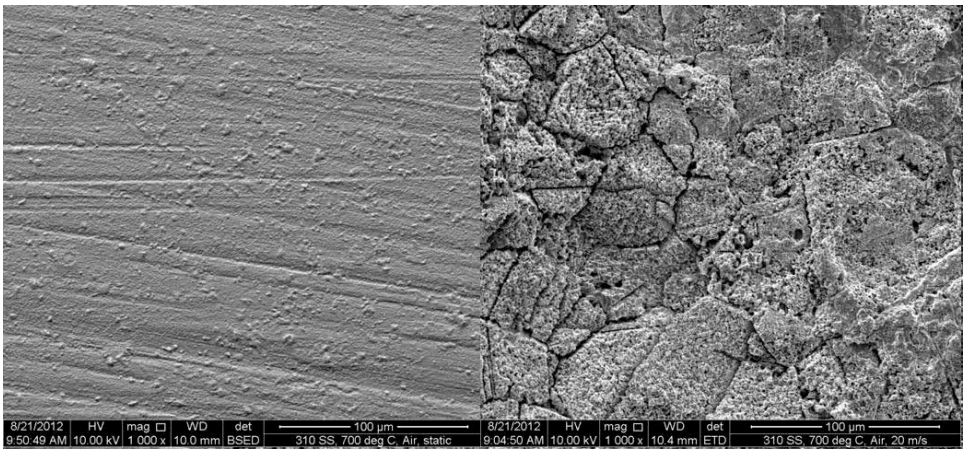

Fig 5. The image on the left shows a 310 SS corrosion sample surface, while the image on the right shows a 310 SS erosion-corrosion sample. Both samples were exposed at 700 °C to air.

The Haynes 230 erosion-corrosion samples did not have the same thin attached scale layer as the 310 SS. After the loose surface scale was removed during cleaning it showed, Fig 6, a mixture of the deformation platelets with a mixture of fine corrosion scale.

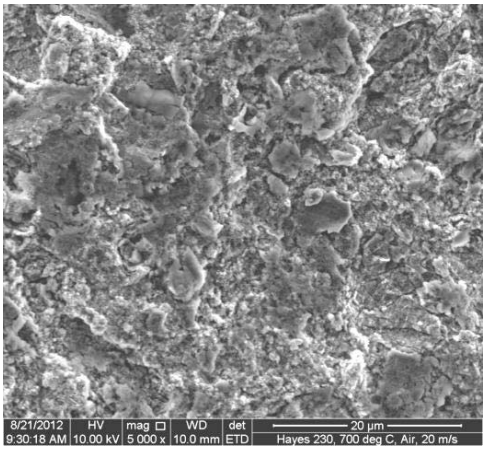

Fig 6. The surface of a Haynes 230 eroded in air at 700 °C. This shows a mixture of impact platelets and corrosion scale.

3.1.3 700 °C in combustion gas tests

The samples tested in the combustion gas at 700 °C showed different adherent scales than those tested in air at 700 °C. On the 310 SS corrosion sample, Fig 7, for example there was an adherent scale that masked any of the original machining marks seen in the 700 °C air case. The surface of the erosion-corrosion sample didn't show any of the cracking seen in the 700 °C air case. A cross-section view of the corrosion sample, Fig 8, shows the surface with minimal grain boundary attack. It appears that most of the scale that had formed during testing was removed in the cleaning process. The remaining scale is 3-4 µm thick. A cross-section view of the erosion-corrosion sample, Fig 9, shows at least 4 or 5 different layers of tightly adherent scale. In this case the scale layer is 20-30 µm thick. This shows the effect of the impacting abrasive can have on the development of the

surface scale. Analysis of surface scales, Table 2, shows a thin lower scale layer for the corrosion sample was largely iron scale and the upper scale was chrome scale. For the erosion-corrosion sample, Table 3, this was reversed with the lower scales being chrome scale while the upper most was mostly iron.

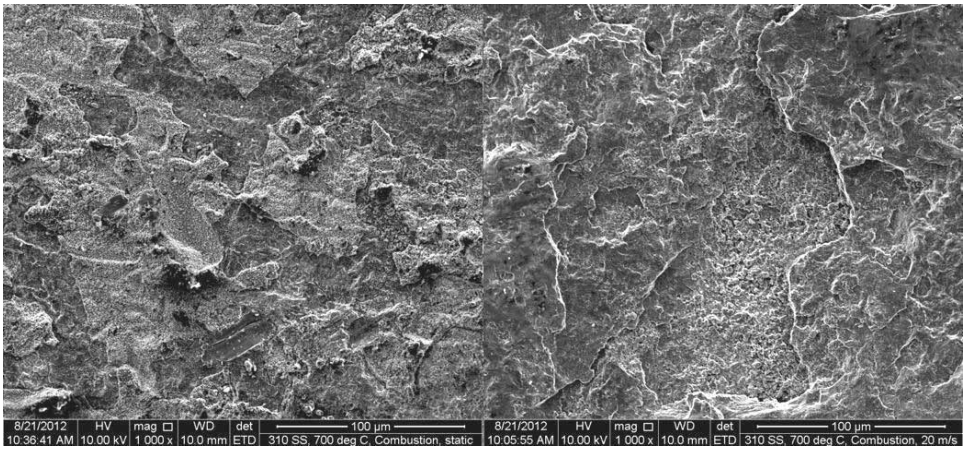

Fig 7. The image on the left shows a 310 SS corrosion sample surface, while the image on the right shows a 310 SS erosion-corrosion sample. Both samples were exposed at 700 °C to a combustion gas.

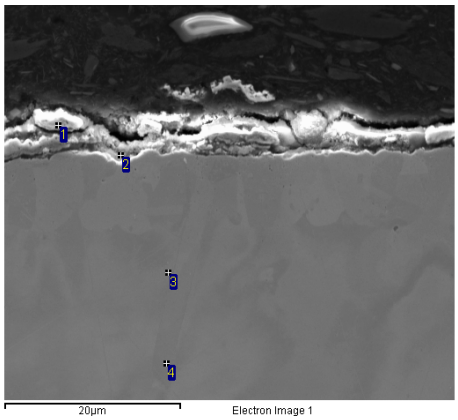

Fig 8. Cross-section of a corroded 310 SS sample tested at 700 °C in a combustion gas. The numbers refer to the location of chemical analysis points found in Table 2.

Location	Cr	Fe	Ni	Si	O
1	70.5	5.79	0.52	4.7	18.5
2	23.2	29.3	9.54	10.6	27.4
3	23.3	51.4	24.3	0.40	0.55
4	24.4	50.1	24.6	0.51	0.40

All results in mass %.

Table 2. Spot EDS chemical analysis results for a 310 SS corrosion sample.

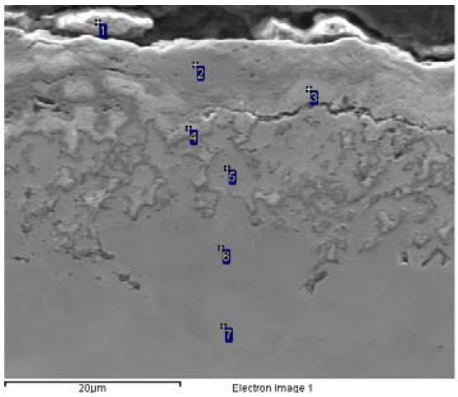

Fig 9. Cross-section of an eroded/corroded 310 SS sample tested at 700 °C in a combustion gas. The numbers refer to the location of chemical analysis points found in Table 3.

Location	Cr	Fe	Ni	Si	O
1	22.7	41.8	1.60	4.87	29.1
2	36.5	37.4	0.85	0.30	24.9
3	64.8	0	0.72	0.15	34.6
4	58.8	9.06	8.41	0.50	23.2
5	9.00	47.6	42.7	0.25	0.41
6	17.9	54.5	26.2	0.60	0.78
7	25.9	50.0	23.1	0.70	0.28

All results in mass %.

Table 3. Spot EDS chemical analysis results for a 310 SS erosion-corrosion sample.

The Hayes 230 showed a thinner adherent scale layer than the 310 SS. As shown in Fig 10, there are still signs of the original machining marks on the corrosion sample. The erosion-corrosion sample shows deformation of the surface through the scale layer. This is more easily seen in the backscatter image of the sample; however, it does not reveal the thin platelet layers of deformed metal shown in the secondary electron image. The analysis of the cross-section seen in Fig 11, shows that the corrosion sample surface scale is largely chrome oxide with traces of W detected (Table 4). The cross-section shows some of the remaining loosely attached scale. The remaining tightly attached scale is ~1 µm thick. There also appears to be some grain boundary attack. There is some internal corrosion, following the grain boundaries, penetrating several µm. The erosion-corrosion cross-section, seen in Fig 12, shows substantial amounts of W in the chrome scale, as can be given in Table 5. The scale, in the case of the erosion-corrosion sample, was ~2-4 µm thick. Again there was internal oxidation, but in this case it did not seem to follow the grain boundaries. In most cases of the alloys studied here, only a small about of nickel was found at the surface. In the case of the Haynes 230, ~20-30 mass % nickel, it was associated with the scale surface.

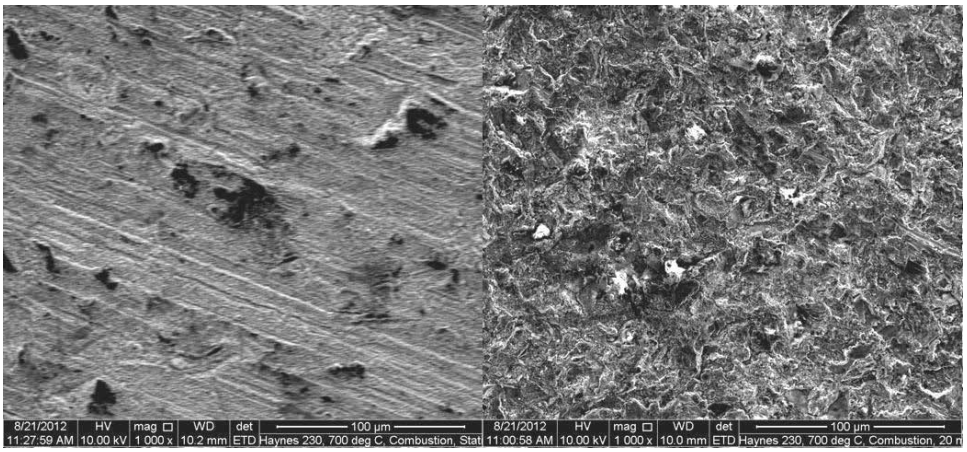

Fig 10. The image on the left shows a Hayes 230 corrosion sample surface, while the image on the right shows a Haynes 230 erosion-corrosion sample. Both samples were exposed at 700 °C to a combustion gas.

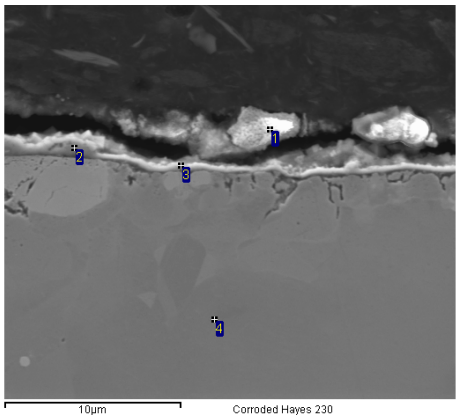

Fig 11. Cross-section of a corroded Haynes 230 sample tested at 700 °C in a combustion gas. The numbers refer to the location of chemical analysis points found in Table 4.

Location	Cr	Ni	W	Si	O
1	38.3	1.60	0	7.96	52.1
2	68.2	0.96	0.92	0	29.9
3	57.2	7.85	6.60	0	28.4
4	16.7	68.2	14.4	0	0.62

All results in mass %.

Table 4. Spot EDS chemical analysis results for a Haynes 230 corrosion sample.

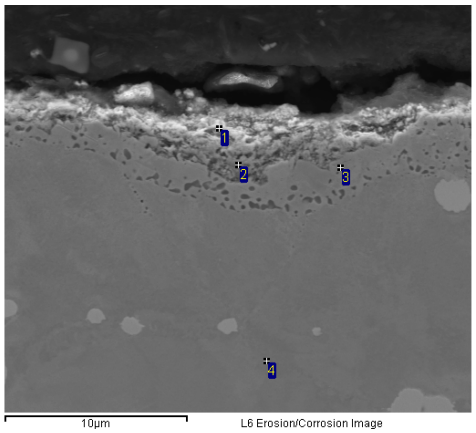

Fig 12. Cross-section of an eroded/corroded Haynes 230 sample tested at 700 °C in a combustion gas. The numbers refer to the location of chemical analysis points found in Table 5.

Location	Cr	Ni	W	Fe	O
1	14.6	21.7	38.3	4.75	20.7
2	20.3	31.8	23.7	4.47	19.8
3	0	85.5	14.1	0	0.48
4	19.5	65.5	15.0	0	0.08

All results in mass %.

Table 5. Spot EDS chemical analysis results for a Haynes 230 erosion-corrosion sample.

The Incoloy 800 corrosion sample, in Fig 13, was still quite clean after exposure, showing the original machining marks and little scale. The cross-section image of the corrosion sample, Fig 14, confirms the thin adherent scale layer, with some possible internal corrosion. This thin scale was primarily chrome and O, with the composition of CrO_3. The erosion-corrosion sample shows a tightly adhered scale with the imprint of the impact deformed base metal showing through. The deformed impact edges were no longer sharply defined after the exposure. The cross-section image of the erosion-corrosion sample, Fig 15, shows a fairly thick, 20-25 µm, scale. The outer most composition is mostly an iron scale. Lower level compositions show mostly chrome scale. This image also shows internal oxidation of at least 20-25 µm deep. EDS of the surface showed some silica, that did not show up in the cross-section.

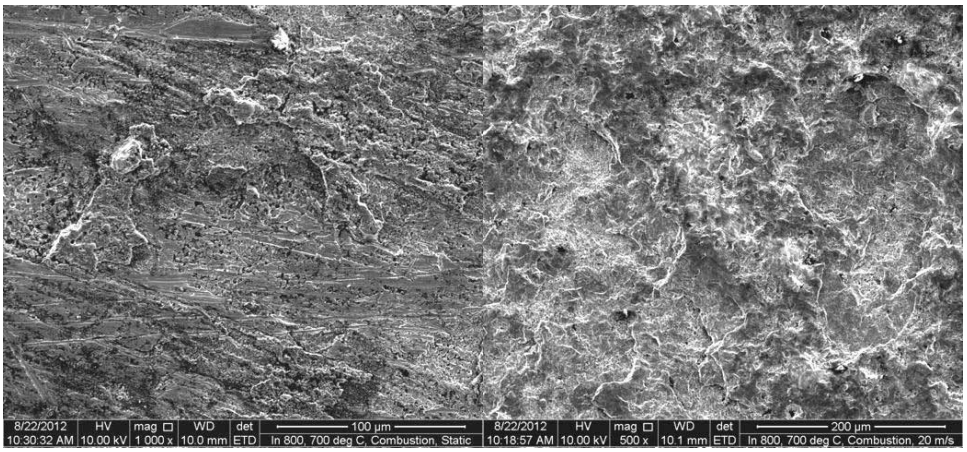

Fig 13. The image on the left shows an Incoloy 800 corrosion sample surface, while the image on the right shows an Incoloy 800 erosion-corrosion sample. Both samples were exposed at 700 °C to a combustion gas.

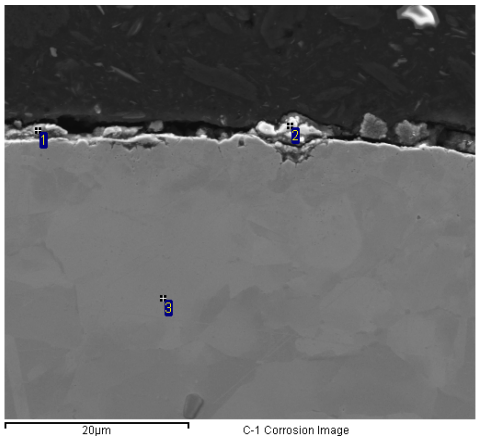

Fig 14. Cross-section of a corroded Incoloy 800 sample tested at 700 °C in a combustion gas. The numbers refer to the location of chemical analysis points found in Table 6.

Location	Cr	Fe	Ni	O
1	41.3	8.74	3.16	46.8
2	67.6	0	0.25	32.2
3	19.7	42.6	37.6	0.14

All results in mass %.

Table 6. Spot EDS chemical analysis results for an Incoloy 800 corrosion sample.

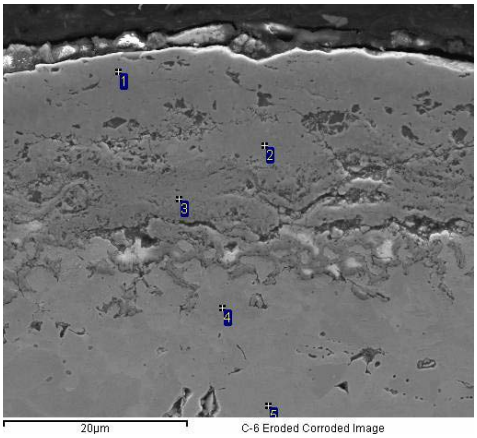

Fig 15. Cross-section of an eroded/corroded Incoloy 800 sample tested at 700 °C in a combustion gas. The numbers refer to the location of chemical analysis points found in Table 7.

Location	Cr	Fe	Ni	O
1	20.0	59.6	0	20.5
2	17.4	53.0	5.11	24.5
3	51.9	24.2	0	23.9
4	21.3	41.8	36.1	0.76
5	15.5	43.4	40.6	0.59

All results in mass %.

Table 7. Spot EDS chemical analysis results for an Incoloy 800 erosion-corrosion sample.

Examination of Fe_3Al, like the Haynes 230, showed only a very thin scale layer on the corrosion sample surface, (Fig 16). The original machining marks are still visible on the surface. The erosion-corrosion surface shows a mixture of mechanical erosion damage and scale. Analysis of the corrosion surface shows oxygen associated with aluminum. The iron concentration is fairly uniform across the surface. There are iron based eruptions from the surface. The erosion-corrosion surface again shows the oxygen associated with aluminum. In this case the iron and the aluminum oxides have formed as distinct separate areas.

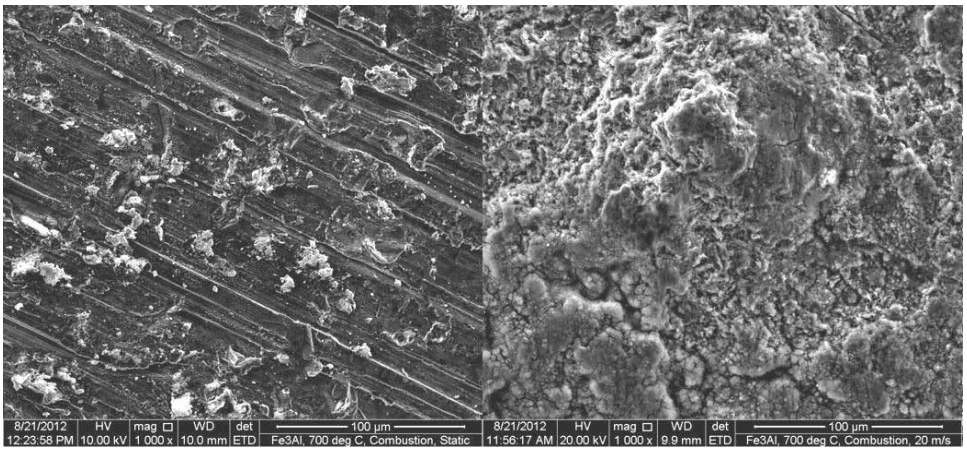

Fig 16. The image on the left show a Fe_3Al corrosion sample surface, while the image on the right shows a Fe_3Al erosion-corrosion sample. Both samples were exposed at 700 °C to a combustion gas.

3.2 Gravimetric measurements

Since both static corrosion samples and moving erosion-corrosion samples were run, a calculation of the corrosion, erosion (with erosion enhanced corrosion), and total erosion-corrosion rate could be made.

Corrosive loss was calculated by measuring the mass change of the corrosion sample (ΔM_c) and then subtracting the mass change of the stub (ΔS_c). The loss rate, in mm/y, was the mass change multiplied by 8760 hours in a year, and then divided by the product of sample area, density of the sample, and test time. Mass gains were seen, due to development of metal scale on the surface of the test specimens.

$$L_c = \frac{(\Delta M_c - \Delta S_c) * 8760}{A * d * t}$$

Where L_C is loss due to corrosion

ΔM_c is the sample mass change due to corrosion.

ΔS_c is the stub mass change due to corrosion.

A is the total area of the sample.

d is the alloy's density.

t is the test time, in this case 120 hr.

Table 8 shows the gravimetric results for the corrosion testing. At room temperature, as expected, the corrosion is near zero. At 700 °C in an air environment both the 310 SS and the Haynes 230 had a substantial mass gain due to the development of adherent scales. At 700 °C, in the combustion gas environment, the scales formed were not as protective. The 310 SS, 304 SS, and the Incoloy 800 showed small mass gains, while the Haynes 230, Nitronic 30 and the Fe_3Al samples showed mass loss. The 2¼Cr 1Mo sample corroded so quickly, at over 7 mm/y, it would be unusable at this temperature.

Conditions		Alloy, corrosion loss in mm/y						
Temp, °C	Atmosphere	310 SS	304 SS	2¼Cr 1Mo	In 800	Haynes 230	Nitronic 30	Fe_3Al
Room	Nitrogen	0.003	0.002	-0.001	0.001	-0.001	-0.001	-0.001
700	Air	-2.53	-	-	-	-3.39	-	-
700	Combustion	-0.25	-.12	7.33	-0.25	0.17	1.26	0.54

Note: the "-" values are mass gains due to scale formation

Table 8. Corrosion loss for alloys tested at various temperatures, in mm/y.

The erosive (with erosion enhanced corrosion) loss was calculated using a similar formula. The measured mass change due to corrosion for an alloy was subtracted from the measure mass loss of each erosion-corrosion sample. This was defined as the mass change due to erosion (with erosion enhanced corrosion). This was multiplied by 8760 hours in a year and then divided by the product of erosion area, density of the sample, and by the erosion-corrosion test time.

$$L_e = \frac{(\Delta M_e - \Delta M_c) * 8760}{A' * d * t}$$

Where L_e is loss due to erosion (plus erosion enhanced corrosion).
ΔM_e is the sample mass change due to erosion-corrosion.
A' is the area of the sample that was eroded.

Table 9 shows the calculated erosion rates (plus erosion enhanced corrosion) for the alloys tested. The room temperature erosion rate between various iron and nickel based alloys is quite similar, as has been reported by others. At 700 °C in air, both the 310 SS and Haynes 230 show a high erosion rate. At 700 °C, in the combustion gas environment, all the alloys are showing a moderate mass loss rate. The Nitronic 30 shows an interestingly low erosion rate in these conditions.

Conditions		Alloy, erosion loss in mm/y						
Temp, °C	Atmosphere	310 SS	304 SS	2¼Cr 1Mo	In 800	Haynes 230	Nitronic 30	Fe_3Al
Room	Nitrogen	0.215	0.217	0.070	0.183	0.211	0.138	0.070
700	Air	4.29	-	-	-	3.12	-	
700	Combustion	1.65	1.49	24.14	2.40	2.71	0.28	0.69

Table 9. Erosion plus erosion enhanced corrosion loss for alloys tested at various temperatures

Table 10 shows the total erosion-corrosion loss rate which results of combining the corrosion with the erosion (with erosion enhanced corrosion) rates. Again the room temperature total erosion-corrosion loss rates are approximately the erosion rates, since the alloys did not see corrosion at room temperature. The row totals for the 700 °C in air show a high rate for the 310 SS steel. The table shows in an apparent material gain for the Haynes 230. The material gain for this condition is because the metal mass loss due to erosion is being reduced by the corrosion mass gain process taking place. This has been

reported previously [18, 20], again at low velocities, and can be attributed to either the corrosion scale being harder and more erosion resistant than the base metal or the erosion process densifying the corrosion layer. The densified surface scale may retard gas diffusion through the scale, which helps limit further corrosion. One area of possible inaccuracy is that the corrosion rates are measured using static corrosion samples, while the erosion-corrosion samples are experiencing corrosion, but in moving gas. Literature indicates corrosion on a still sample and a sample moving through a gas will likely be different, but this is has not been well studied for the various alloys.

One interesting observation is, other than the 2¼Cr 1Mo which is recognized as unsuitable for 700 °C+ service, the nickel based Haynes 230 and the high nickel Incoloy 800 have the highest mass loss rates. This may warrant further investigation, in that many of the advanced ultra-super-critical PC power plants are expected to use high nickel alloys extensively.

Conditions		Alloy, total erosion-corrosion loss in mm/y						
Temp, °C	Atmosphere	310 SS	304 SS	2¼Cr 1Mo	In 800	Haynes 230	Nitronic 30	Fe_3Al
Room	Nitrogen	0.218	0.219	0.070	0.184	0.209	0.137	0.069
700	Air	1.77	-	-	-	-.263	-	-
700	Combustion	1.40	1.37	31.46	2.16	2.88	1.55	1.49

Table 10. Total erosion-corrosion loss rate for alloys tested at various temperatures.

4. Conclusion

A variety of metal alloys have been evaluated for corrosion and erosion-corrosion resistance at room temperature and 700 °C in both air and a combustion gas environment at low gas velocities. These tests show that an alloy's erosion (with erosion enhanced corrosion) is at least as important as its corrosion rate at high temperatures. While at low velocities the erosive process will not completely remove the corrosion scale, the tests show that the outer corrosion scale can be affected by the erosive process. Further it was seen that high temperature erosion-corrosion resistance in air is not a predictor of high temperature erosion-corrosion resistance in a combustion gas environment.

While gravimetric results show that a high alloy concentration of chrome is important to the erosion-corrosion resistance of these alloys, EDS results show that the outer scales tend to be more iron rich than chrome. High nickel alloys, such as Incoloy 800 and Haynes 230 did not perform as well as more conventional metals like 304 and 310 SS. More work needs to be done on the concentration effects of secondary, corrosive, gases such as HCl and SO_2.

5. Disclaimer

information, apparatus, product, or process disclosed, or represents that its use would not infringe privately owned rights. Reference herein to any specific commercial product, process, or service by trade name, trademark, manufacturer, or otherwise does not necessarily constitute or imply its endorsement, recommendation, or favoring by the United States Government or any agency thereof. The views and opinions of authors expressed herein do not necessarily state or reflect those of the United States Government or any agency thereof.

6. References

[1] A. Levy, V., National Association of Corrosion Engineers. Technical Practices Committee T-2, Proceedings: Corrosion-erosion-wear of materials in emerging fossil energy systems, NACE International, Berkeley, California, 1982.

[2] A. Levy, V., National Association Corrosion Engineers. Group Committee T-2, Corrosion-erosion-wear of materials at elevated temperatures, NACE International, Houston TX, 1987.

[3] A. Levy, V., Proceedings: Corrosion-erosion-wear of materials at elevated temperatures, NACE International, Houston TX, 1991.

[4] I.G. Wright, V.K. Sethi, A.J. Markworth, A generalized description of the simultaneous processes of scale growth by high-temperature oxidation and removal by erosive impact, Wear, 186-187, Part 1 (0) (1995) 230-237.

[5] A. Drotlew, P. Christodoulou, V. Gutowski, Erosion of ferritic fe-cr-c cast alloys at elevated temperatures, Wear, 211 (1) (1997) 120-128.

[6] E. Raask, Tube erosion by ash impaction, Wear, 13 (4–5) (1969) 301-315.

[7] E. Raask, Erosion wear in coal utilization, Hemisphere Pub. Corp., 1988.

[8] J. Stringer, Practical experience with wastage at elevated temperatures in coal combustion systems, Wear, 186-187, Part 1 (0) (1995) 11-27.

[9] M. Suckling, C. Allen, Critical variables in high temperature erosive wear, Wear, 203–204 (0) (1997) 528-536.

[10] G. Sorell, Elevated temperature erosion-corrosion of alloys in sulfidizing gas-solid streams: Parametric studies, in: A.V. Levy (Ed.) Corrosion-Erosion-Wear of Materials at Elevated Temperatures, Berkeley, CA, 1986, 396.

[11] W. Bakker, Materials guidelines for gasification plants, EPRI, Palo Alto, CA, 1998.

[12] D.J. Stephenson, J.R. Nicholls, Modelling the influence of surface oxidation on high temperature erosion, Wear, 186–187, Part 1 (0) (1995) 284-290.

[13] R. Romanosky, P. Rawls, M.L. Santella, Materials for advanced ultra-supercritical steam power plants, (2011), http://www.netl.doe.gov/publications/factsheets/project/feaa061.pdf, Aug 23, 2012.

[14] J.R. Nicholls, Laboratory studies of erosion-corrosion processes under oxidising and oxidising/sulphidising conditions, Materials at High temperatures, 14 (3) (1997) 18.

[15] P.L. Daniel, Corrosive species in rdf-fired boilers, in: A. Levy, V. (Ed.) Corrosion-Erosion-Wear of Materials at Elevated Temperatures, NACE, Berkeley, CA, 1990.
[16] S.C. Stultz, J.B. Kitto, Steam its generation and use, 40th edition, The Babcock & Wilcock Company, Barberton, Ohio, 1992.
[17] R.O. Scattergood, Review of erosion test methodologies, in: A.V. Levy (Ed.) Corrosion-Erosion-Wear of Mateirals at Elevated Temperatures, NACE, Berkeley CA, 1990, 13.
[18] J. Tylczak, T. Adler, J. Rawers, Abrasion and erosion testing of materials used in power production from coal, 20th Annual International Pittsburgh Coal Conf, Pittsburgh, PA, 2003, 13.
[19] I.M. Hutchings, A model for the erosion of metals by spherical particles at normal incidence, Wear, 70 (3) (1981) 269-281.
[20] F.H. Stott, M.M. Stack, G.C. Wood, The role of oxides in the erosino-corrosion of alloys, in: A.V. Levy (Ed.) Corrosion-Errosion -Wear of Materials at Elevated Temperatures, NACE Int, Berkeley, CA, 1990.